

Measurement of $d\sigma/dy$ of Drell-Yan e^+e^- pairs in the Z Mass Region from $p\bar{p}$ Collisions at $\sqrt{s}=1.96$ TeV

T. Aaltonen,²⁴ J. Adelman,¹⁴ B. Álvarez González^{w,12} S. Amerio^{ee,44} D. Amidei,³⁵ A. Anastassov,³⁹ A. Annovi,²⁰ J. Antos,¹⁵ G. Apollinari,¹⁸ J. Appel,¹⁸ A. Apresyan,⁴⁹ T. Arisawa,⁵⁸ A. Artikov,¹⁶ J. Asaadi,⁵⁴ W. Ashmanskas,¹⁸ A. Attal,⁴ A. Aurisano,⁵⁴ F. Azfar,⁴³ W. Badgett,¹⁸ A. Barbaro-Galtieri,²⁹ V.E. Barnes,⁴⁹ B.A. Barnett,²⁶ P. Barria^{gg,47} P. Bartos,¹⁵ G. Bauer,³³ P.-H. Beauchemin,³⁴ F. Bedeschi,⁴⁷ D. Beecher,³¹ S. Behari,²⁶ G. Bellettini^{ff,47} J. Bellinger,⁶⁰ D. Benjamin,¹⁷ A. Beretvas,¹⁸ A. Bhatti,⁵¹ M. Binkley*,¹⁸ D. Bisello^{ee,44} I. Bizjak^{kk,31} R.E. Blair,² C. Blocker,⁷ B. Blumenfeld,²⁶ A. Bocci,¹⁷ A. Bodek,⁵⁰ V. Boisvert,⁵⁰ D. Bortoletto,⁴⁹ J. Boudreau,⁴⁸ A. Boveia,¹¹ B. Brau^{a,11} A. Bridgeman,²⁵ L. Brigliadori^{dd,6} C. Bromberg,³⁶ E. Brubaker,¹⁴ J. Budagov,¹⁶ H.S. Budd,⁵⁰ S. Budd,²⁵ K. Burkett,¹⁸ G. Busetto^{ee,44} P. Bussey,²² A. Buzatu,³⁴ K. L. Byrum,² S. Cabrera^{y,17} C. Calancha,³² S. Camarda,⁴ M. Campanelli,³¹ M. Campbell,³⁵ F. Canelli^{14,18} A. Canepa,⁴⁶ B. Carls,²⁵ D. Carlsmith,⁶⁰ R. Carosi,⁴⁷ S. Carrillo^{n,19} S. Carron,¹⁸ B. Casal,¹² M. Casarsa,¹⁸ A. Castro^{dd,6} P. Catastini^{gg,47} D. Cauz,⁵⁵ V. Cavaliere^{gg,47} M. Cavalli-Sforza,⁴ A. Cerri,²⁹ L. Cerrito^{q,31} S.H. Chang,²⁸ Y.C. Chen,¹ M. Chertok,⁸ G. Chiarelli,⁴⁷ G. Chlachidze,¹⁸ F. Chlebana,¹⁸ K. Cho,²⁸ D. Chokheli,¹⁶ J.P. Chou,²³ K. Chung^{o,18} W.H. Chung,⁶⁰ Y.S. Chung,⁵⁰ T. Chwalek,²⁷ C.I. Ciobanu,⁴⁵ M.A. Ciocci^{gg,47} A. Clark,²¹ D. Clark,⁷ G. Compostella,⁴⁴ M.E. Convery,¹⁸ J. Conway,⁸ M. Corbo,⁴⁵ M. Cordelli,²⁰ C.A. Cox,⁸ D.J. Cox,⁸ F. Crescioli^{ff,47} C. Cuenca Almenar,⁶¹ J. Cuevas^{w,12} R. Culbertson,¹⁸ J.C. Cully,³⁵ D. Dagenhart,¹⁸ N. d'Ascenzo^{v,45} M. Datta,¹⁸ T. Davies,²² P. de Barbaro,⁵⁰ S. De Cecco,⁵² A. Deisher,²⁹ G. De Lorenzo,⁴ M. Dell'Orso^{ff,47} C. Deluca,⁴ L. Demortier,⁵¹ J. Deng^{f,17} M. Deninno,⁶ M. d'Errico^{ee,44} A. Di Canto^{ff,47} B. Di Ruzza,⁴⁷ J.R. Dittmann,⁵ M. D'Onofrio,⁴ S. Donati^{ff,47} P. Dong,¹⁸ T. Dorigo,⁴⁴ S. Dube,⁵³ K. Ebina,⁵⁸ A. Elagin,⁵⁴ R. Erbacher,⁸ D. Errede,²⁵ S. Errede,²⁵ N. Ershaidat^{cc,45} R. Eusebi,⁵⁴ H.C. Fang,²⁹ S. Farrington,⁴³ W.T. Fedorko,¹⁴ R.G. Feild,⁶¹ M. Feindt,²⁷ J.P. Fernandez,³² C. Ferrazza^{hh,47} R. Field,¹⁹ G. Flanagan^{s,49} R. Forrest,⁸ M.J. Frank,⁵ M. Franklin,²³ J.C. Freeman,¹⁸ I. Furic,¹⁹ M. Gallinaro,⁵¹ J. Galyardt,¹³ F. Garberson,¹¹ J.E. Garcia,²¹ A.F. Garfinkel,⁴⁹ P. Garosi^{gg,47} H. Gerberich,²⁵ D. Gerdes,³⁵ A. Gessler,²⁷ S. Giagu^{ii,52} V. Giakoumopoulou,³ P. Giannetti,⁴⁷ K. Gibson,⁴⁸ J.L. Gimmell,⁵⁰ C.M. Ginsburg,¹⁸ N. Giokaris,³ M. Giordani^{jj,55} P. Giromini,²⁰ M. Giunta,⁴⁷ G. Giurgiu,²⁶ V. Glagolev,¹⁶ D. Glenzinski,¹⁸ M. Gold,³⁸ N. Goldschmidt,¹⁹ A. Golossanov,¹⁸ G. Gomez,¹² G. Gomez-Ceballos,³³ M. Goncharov,³³ O. González,³² I. Gorelov,³⁸ A.T. Goshaw,¹⁷ K. Goulianos,⁵¹ A. Gresele^{ee,44} S. Grinstein,⁴ C. Grosso-Pilcher,¹⁴ R.C. Group,¹⁸ U. Grundler,²⁵ J. Guimaraes da Costa,²³ Z. Gunay-Unalan,³⁶ C. Haber,²⁹ S.R. Hahn,¹⁸ E. Halkiadakis,⁵³ B.-Y. Han,⁵⁰ J.Y. Han,⁵⁰ F. Happacher,²⁰ K. Hara,⁵⁶ D. Hare,⁵³ M. Hare,⁵⁷ R.F. Harr,⁵⁹ M. Hartz,⁴⁸ K. Hatakeyama,⁵ C. Hays,⁴³ M. Heck,²⁷ J. Heinrich,⁴⁶ M. Herndon,⁶⁰ J. Heuser,²⁷ S. Hewamanage,⁵ D. Hidas,⁵³ C.S. Hill^{c,11} D. Hirschbuehl,²⁷ A. Hocker,¹⁸ S. Hou,¹ M. Houlden,³⁰ S.-C. Hsu,²⁹ R.E. Hughes,⁴⁰ M. Hurwitz,¹⁴ U. Husemann,⁶¹ M. Hussein,³⁶ J. Huston,³⁶ J. Incandela,¹¹ G. Introzzi,⁴⁷ M. Iori^{ii,52} A. Ivanov^{p,8} E. James,¹⁸ D. Jang,¹³ B. Jayatilaka,¹⁷ E.J. Jeon,²⁸ M.K. Jha,⁶ S. Jindariani,¹⁸ W. Johnson,⁸ M. Jones,⁴⁹ K.K. Joo,²⁸ S.Y. Jun,¹³ J.E. Jung,²⁸ T.R. Junk,¹⁸ T. Kamon,⁵⁴ D. Kar,¹⁹ P.E. Karchin,⁵⁹ Y. Kato^{m,42} R. Kephart,¹⁸ W. Ketchum,¹⁴ J. Keung,⁴⁶ V. Khotilovich,⁵⁴ B. Kilminster,¹⁸ D.H. Kim,²⁸ H.S. Kim,²⁸ H.W. Kim,²⁸ J.E. Kim,²⁸ M.J. Kim,²⁰ S.B. Kim,²⁸ S.H. Kim,⁵⁶ Y.K. Kim,¹⁴ N. Kimura,⁵⁸ L. Kirsch,⁷ S. Klimenko,¹⁹ K. Kondo,⁵⁸ D.J. Kong,²⁸ J. Konigsberg,¹⁹ A. Korytov,¹⁹ A.V. Kotwal,¹⁷ M. Kreps,²⁷ J. Kroll,⁴⁶ D. Krop,¹⁴ N. Krumnack,⁵ M. Kruse,¹⁷ V. Krutelyov,¹¹ T. Kuhr,²⁷ N.P. Kulkarni,⁵⁹ M. Kurata,⁵⁶ S. Kwang,¹⁴ A.T. Laasanen,⁴⁹ S. Lami,⁴⁷ S. Lammel,¹⁸ M. Lancaster,³¹ R.L. Lander,⁸ K. Lannon^{u,40} A. Lath,⁵³ G. Latino^{gg,47} I. Lazzizzera^{ee,44} T. LeCompte,² E. Lee,⁵⁴ H.S. Lee,¹⁴ J.S. Lee,²⁸ S.W. Lee^{x,54} S. Leone,⁴⁷ J.D. Lewis,¹⁸ C.-J. Lin,²⁹ J. Linacre,⁴³ M. Lindgren,¹⁸ E. Lipeles,⁴⁶ A. Lister,²¹ D.O. Litvintsev,¹⁸ C. Liu,⁴⁸ T. Liu,¹⁸ N.S. Lockyer,⁴⁶ A. Loginov,⁶¹ L. Lovas,¹⁵ D. Lucchesi^{ee,44} J. Lueck,²⁷ P. Lujan,²⁹ P. Lukens,¹⁸ G. Lungu,⁵¹ J. Lys,²⁹ R. Lysak,¹⁵ D. MacQueen,³⁴ R. Madrak,¹⁸ K. Maeshima,¹⁸ K. Makhoul,³³ P. Maksimovic,²⁶ S. Malde,⁴³ S. Malik,³¹ G. Manca^{e,30} A. Manousakis-Katsikakis,³ F. Margaroli,⁴⁹ C. Marino,²⁷ C.P. Marino,²⁵ A. Martin,⁶¹ V. Martin^{k,22} M. Martínez,⁴ R. Martínez-Ballarín,³² P. Mastrandrea,⁵² M. Mathis,²⁶ M.E. Mattson,⁵⁹ P. Mazzanti,⁶ K.S. McFarland,⁵⁰ P. McIntyre,⁵⁴ R. McNulty^{j,30} A. Mehta,³⁰ P. Mehtala,²⁴ A. Menzione,⁴⁷ C. Mesropian,⁵¹ T. Miao,¹⁸ D. Mietlicki,³⁵ N. Miladinovic,⁷ R. Miller,³⁶ C. Mills,²³ M. Milnik,²⁷ A. Mitra,¹ G. Mitselmakher,¹⁹ H. Miyake,⁵⁶ S. Moed,²³ N. Moggi,⁶ M.N. Mondragon^{n,18} C.S. Moon,²⁸ R. Moore,¹⁸ M.J. Morello,⁴⁷ J. Morlock,²⁷ P. Movilla Fernandez,¹⁸ J. Mülmenstädt,²⁹ A. Mukherjee,¹⁸ Th. Muller,²⁷ P. Murat,¹⁸ M. Mussini^{dd,6} J. Nachtman^{o,18} Y. Nagai,⁵⁶ J. Naganoma,⁵⁶ K. Nakamura,⁵⁶ I. Nakano,⁴¹ A. Napier,⁵⁷ J. Nett,⁶⁰ C. Neu^{aa,46} M.S. Neubauer,²⁵ S. Neubauer,²⁷ J. Nielsen^{g,29} L. Nodulman,² M. Norman,¹⁰ O. Norniella,²⁵ E. Nurse,³¹ L. Oakes,⁴³ S.H. Oh,¹⁷ Y.D. Oh,²⁸ I. Oksuzian,¹⁹ T. Okusawa,⁴² R. Orava,²⁴ K. Osterberg,²⁴ S. Pagan Griso^{ee,44}

C. Pagliarone,⁵⁵ E. Palencia,¹⁸ V. Papadimitriou,¹⁸ A. Papaikonomou,²⁷ A.A. Paramanov,² B. Parks,⁴⁰ S. Pashapour,³⁴ J. Patrick,¹⁸ G. Pauletta^{jj},⁵⁵ M. Paulini,¹³ C. Paus,³³ T. Peiffer,²⁷ D.E. Pellett,⁸ A. Penzo,⁵⁵ T.J. Phillips,¹⁷ G. Piacentino,⁴⁷ E. Pianori,⁴⁶ L. Pinera,¹⁹ K. Pitts,²⁵ C. Plager,⁹ L. Pondrom,⁶⁰ K. Potamianos,⁴⁹ O. Poukhov*,¹⁶ F. Prokoshin^z,¹⁶ A. Pronko,¹⁸ F. Ptohosⁱ,¹⁸ E. Pueschel,¹³ G. Punzi^{ff},⁴⁷ J. Pursley,⁶⁰ J. Rademacker^c,⁴³ A. Rahaman,⁴⁸ V. Ramakrishnan,⁶⁰ N. Ranjan,⁴⁹ I. Redondo,³² P. Renton,⁴³ M. Renz,²⁷ M. Rescigno,⁵² S. Richter,²⁷ F. Rimondi^{dd},⁶ L. Ristori,⁴⁷ A. Robson,²² T. Rodrigo,¹² T. Rodriguez,⁴⁶ E. Rogers,²⁵ S. Rolli,⁵⁷ R. Roser,¹⁸ M. Rossi,⁵⁵ R. Rossin,¹¹ P. Roy,³⁴ A. Ruiz,¹² J. Russ,¹³ V. Rusu,¹⁸ B. Rutherford,¹⁸ H. Saarikko,²⁴ A. Safonov,⁵⁴ W.K. Sakumoto,⁵⁰ L. Santi^{jj},⁵⁵ L. Sartori,⁴⁷ K. Sato,⁵⁶ V. Saveliev^v,⁴⁵ A. Savoy-Navarro,⁴⁵ P. Schlabach,¹⁸ A. Schmidt,²⁷ E.E. Schmidt,¹⁸ M.A. Schmidt,¹⁴ M.P. Schmidt*,⁶¹ M. Schmitt,³⁹ T. Schwarz,⁸ L. Scodellaro,¹² A. Scribano^{gg},⁴⁷ F. Scuri,⁴⁷ A. Sedov,⁴⁹ S. Seidel,³⁸ Y. Seiya,⁴² A. Semenov,¹⁶ L. Sexton-Kennedy,¹⁸ F. Sforza^{ff},⁴⁷ A. Sfyrla,²⁵ S.Z. Shalhout,⁵⁹ T. Shears,³⁰ P.F. Shepard,⁴⁸ M. Shimojima^t,⁵⁶ S. Shiraishi,¹⁴ M. Shochet,¹⁴ Y. Shon,⁶⁰ I. Shreyber,³⁷ A. Simonenko,¹⁶ P. Sinervo,³⁴ A. Sisakyan,¹⁶ A.J. Slaughter,¹⁸ J. Slaunwhite,⁴⁰ K. Sliwa,⁵⁷ J.R. Smith,⁸ F.D. Snider,¹⁸ R. Snihur,³⁴ A. Soha,¹⁸ S. Somalwar,⁵³ V. Sorin,⁴ P. Squillacioti^{gg},⁴⁷ M. Stanitzki,⁶¹ R. St. Denis,²² B. Stelzer,³⁴ O. Stelzer-Chilton,³⁴ D. Stentz,³⁹ J. Strogas,³⁸ G.L. Strycker,³⁵ J.S. Suh,²⁸ A. Sukhanov,¹⁹ I. Suslov,¹⁶ A. Taffard^f,²⁵ R. Takashima,⁴¹ Y. Takeuchi,⁵⁶ R. Tanaka,⁴¹ J. Tang,¹⁴ M. Tecchio,³⁵ P.K. Teng,¹ J. Thom^h,¹⁸ J. Thome,¹³ G.A. Thompson,²⁵ E. Thomson,⁴⁶ P. Tipton,⁶¹ P. Ttito-Guzmán,³² S. Tkaczyk,¹⁸ D. Toback,⁵⁴ S. Tokar,¹⁵ K. Tollefson,³⁶ T. Tomura,⁵⁶ D. Tonelli,¹⁸ S. Torre,²⁰ D. Torretta,¹⁸ P. Totaro^{jj},⁵⁵ M. Trovato^{hh},⁴⁷ S.-Y. Tsai,¹ Y. Tu,⁴⁶ N. Turini^{gg},⁴⁷ F. Ukegawa,⁵⁶ S. Uozumi,²⁸ N. van Remortel^b,²⁴ A. Varganov,³⁵ E. Vataga^{hh},⁴⁷ F. Vázquezⁿ,¹⁹ G. Velev,¹⁸ C. Vellidis,³ M. Vidal,³² I. Vila,¹² R. Vilar,¹² M. Vogel,³⁸ I. Volobouev^x,²⁹ G. Volpi^{ff},⁴⁷ P. Wagner,⁴⁶ R.G. Wagner,² R.L. Wagner,¹⁸ W. Wagner^{bb},²⁷ J. Wagner-Kuhr,²⁷ T. Wakisaka,⁴² R. Wallny,⁹ S.M. Wang,¹ A. Warburton,³⁴ D. Waters,³¹ M. Weinberger,⁵⁴ J. Weinel^t,²⁷ W.C. Wester III,¹⁸ B. Whitehouse,⁵⁷ D. Whiteson^f,⁴⁶ A.B. Wicklund,² E. Wicklund,¹⁸ S. Wilbur,¹⁴ G. Williams,³⁴ H.H. Williams,⁴⁶ P. Wilson,¹⁸ B.L. Winer,⁴⁰ P. Wittich^h,¹⁸ S. Wolbers,¹⁸ C. Wolfe,¹⁴ H. Wolfe,⁴⁰ T. Wright,³⁵ X. Wu,²¹ F. Würthwein,¹⁰ A. Yagil,¹⁰ K. Yamamoto,⁴² J. Yamaoka,¹⁷ U.K. Yang^r,¹⁴ Y.C. Yang,²⁸ W.M. Yao,²⁹ G.P. Yeh,¹⁸ K. Yi^o,¹⁸ J. Yoh,¹⁸ K. Yorita,⁵⁸ T. Yoshida^l,⁴² G.B. Yu,¹⁷ I. Yu,²⁸ S.S. Yu,¹⁸ J.C. Yun,¹⁸ A. Zanetti,⁵⁵ Y. Zeng,¹⁷ X. Zhang,²⁵ Y. Zheng^d,⁹ and S. Zucchelli^{dd}⁶

(CDF Collaboration[†])

¹*Institute of Physics, Academia Sinica, Taipei, Taiwan 11529, Republic of China*

²*Argonne National Laboratory, Argonne, Illinois 60439, USA*

³*University of Athens, 157 71 Athens, Greece*

⁴*Institut de Fisica d'Altes Energies, Universitat Autònoma de Barcelona, E-08193, Bellaterra (Barcelona), Spain*

⁵*Baylor University, Waco, Texas 76798, USA*

⁶*Istituto Nazionale di Fisica Nucleare Bologna, ^{dd}University of Bologna, I-40127 Bologna, Italy*

⁷*Brandeis University, Waltham, Massachusetts 02254, USA*

⁸*University of California, Davis, Davis, California 95616, USA*

⁹*University of California, Los Angeles, Los Angeles, California 90024, USA*

¹⁰*University of California, San Diego, La Jolla, California 92093, USA*

¹¹*University of California, Santa Barbara, Santa Barbara, California 93106, USA*

¹²*Instituto de Fisica de Cantabria, CSIC-University of Cantabria, 39005 Santander, Spain*

¹³*Carnegie Mellon University, Pittsburgh, Pennsylvania 15213, USA*

¹⁴*Enrico Fermi Institute, University of Chicago, Chicago, Illinois 60637, USA*

¹⁵*Comenius University, 842 48 Bratislava, Slovakia; Institute of Experimental Physics, 040 01 Kosice, Slovakia*

¹⁶*Joint Institute for Nuclear Research, RU-141980 Dubna, Russia*

¹⁷*Duke University, Durham, North Carolina 27708, USA*

¹⁸*Fermi National Accelerator Laboratory, Batavia, Illinois 60510, USA*

¹⁹*University of Florida, Gainesville, Florida 32611, USA*

²⁰*Laboratori Nazionali di Frascati, Istituto Nazionale di Fisica Nucleare, I-00044 Frascati, Italy*

²¹*University of Geneva, CH-1211 Geneva 4, Switzerland*

²²*Glasgow University, Glasgow G12 8QQ, United Kingdom*

²³*Harvard University, Cambridge, Massachusetts 02138, USA*

²⁴*Division of High Energy Physics, Department of Physics, University of Helsinki and Helsinki Institute of Physics, FIN-00014, Helsinki, Finland*

²⁵*University of Illinois, Urbana, Illinois 61801, USA*

²⁶*The Johns Hopkins University, Baltimore, Maryland 21218, USA*

²⁷*Institut für Experimentelle Kernphysik, Karlsruhe Institute of Technology, D-76131 Karlsruhe, Germany*

²⁸*Center for High Energy Physics: Kyungpook National University,*

Daegu 702-701, Korea; Seoul National University, Seoul 151-742,

Korea; Sungkyunkwan University, Suwon 440-746,

- Korea; Korea Institute of Science and Technology Information,
Daejeon 305-806, Korea; Chonnam National University, Gwangju 500-757,
Korea; Chonbuk National University, Jeonju 561-756, Korea
- ²⁹Ernest Orlando Lawrence Berkeley National Laboratory, Berkeley, California 94720, USA
- ³⁰University of Liverpool, Liverpool L69 7ZE, United Kingdom
- ³¹University College London, London WC1E 6BT, United Kingdom
- ³²Centro de Investigaciones Energeticas Medioambientales y Tecnologicas, E-28040 Madrid, Spain
- ³³Massachusetts Institute of Technology, Cambridge, Massachusetts 02139, USA
- ³⁴Institute of Particle Physics: McGill University, Montréal, Québec,
Canada H3A 2T8; Simon Fraser University, Burnaby, British Columbia,
Canada V5A 1S6; University of Toronto, Toronto, Ontario,
Canada M5S 1A7; and TRIUMF, Vancouver, British Columbia, Canada V6T 2A3
- ³⁵University of Michigan, Ann Arbor, Michigan 48109, USA
- ³⁶Michigan State University, East Lansing, Michigan 48824, USA
- ³⁷Institution for Theoretical and Experimental Physics, ITEP, Moscow 117259, Russia
- ³⁸University of New Mexico, Albuquerque, New Mexico 87131, USA
- ³⁹Northwestern University, Evanston, Illinois 60208, USA
- ⁴⁰The Ohio State University, Columbus, Ohio 43210, USA
- ⁴¹Okayama University, Okayama 700-8530, Japan
- ⁴²Osaka City University, Osaka 588, Japan
- ⁴³University of Oxford, Oxford OX1 3RH, United Kingdom
- ⁴⁴Istituto Nazionale di Fisica Nucleare, Sezione di Padova-Trento, ^{ee}University of Padova, I-35131 Padova, Italy
- ⁴⁵LPNHE, Universite Pierre et Marie Curie/IN2P3-CNRS, UMR7585, Paris, F-75252 France
- ⁴⁶University of Pennsylvania, Philadelphia, Pennsylvania 19104, USA
- ⁴⁷Istituto Nazionale di Fisica Nucleare Pisa, ^{ff}University of Pisa,
- ^{gg}University of Siena and ^{hh}Scuola Normale Superiore, I-56127 Pisa, Italy
- ⁴⁸University of Pittsburgh, Pittsburgh, Pennsylvania 15260, USA
- ⁴⁹Purdue University, West Lafayette, Indiana 47907, USA
- ⁵⁰University of Rochester, Rochester, New York 14627, USA
- ⁵¹The Rockefeller University, New York, New York 10021, USA
- ⁵²Istituto Nazionale di Fisica Nucleare, Sezione di Roma 1,
ⁱⁱSapienza Università di Roma, I-00185 Roma, Italy
- ⁵³Rutgers University, Piscataway, New Jersey 08855, USA
- ⁵⁴Texas A&M University, College Station, Texas 77843, USA
- ⁵⁵Istituto Nazionale di Fisica Nucleare Trieste/Udine,
I-34100 Trieste, ^{jj}University of Trieste/Udine, I-33100 Udine, Italy
- ⁵⁶University of Tsukuba, Tsukuba, Ibaraki 305, Japan
- ⁵⁷Tufts University, Medford, Massachusetts 02155, USA
- ⁵⁸Waseda University, Tokyo 169, Japan
- ⁵⁹Wayne State University, Detroit, Michigan 48201, USA
- ⁶⁰University of Wisconsin, Madison, Wisconsin 53706, USA
- ⁶¹Yale University, New Haven, Connecticut 06520, USA

We report on a CDF measurement of the total cross section and rapidity distribution, $d\sigma/dy$, for $q\bar{q} \rightarrow \gamma^*/Z \rightarrow e^+e^-$ events in the Z boson mass region ($66 < M_{ee} < 116$ GeV/ c^2) produced in $p\bar{p}$ collisions at $\sqrt{s} = 1.96$ TeV with 2.1 fb^{-1} of integrated luminosity. The measured cross section of 257 ± 16 pb and $d\sigma/dy$ distribution are compared with Next-to-Leading-Order(NLO) and Next-to-Next-to-Leading-Order(NNLO) QCD theory predictions with CTEQ and MRST/MSTW parton distribution functions (PDFs). There is good agreement between the experimental total cross section and $d\sigma/dy$ measurements with theoretical calculations with the most recent NNLO PDFs.

Keywords : Z Boson Rapidity $d\sigma/dy$ PDFs

*Deceased

†With visitors from ^aUniversity of Massachusetts Amherst, Amherst, Massachusetts 01003, ^bUniversiteit Antwerpen, B-2610 Antwerp, Belgium, ^cUniversity of Bristol, Bristol BS8 1TL, United Kingdom, ^dChinese Academy of Sciences, Beijing 100864, China, ^eIstituto Nazionale di Fisica Nucleare, Sezione di Cagliari,

09042 Monserrato (Cagliari), Italy, ^fUniversity of California Irvine, Irvine, CA 92697, ^gUniversity of California Santa Cruz, Santa Cruz, CA 95064, ^hCornell University, Ithaca, NY 14853, ⁱUniversity of Cyprus, Nicosia CY-1678, Cyprus, ^jUniversity College Dublin, Dublin 4, Ireland, ^kUniversity of Edinburgh, Edinburgh EH9 3JZ, United Kingdom, ^lUniversity of Fukui, Fukui City,

I. INTRODUCTION

Accurate predictions using perturbative quantum chromodynamics (QCD) are critical for understanding experimental results at hadron colliders. Such predictions depend on the accuracy of input parton distribution functions (PDFs), which at present cannot be calculated and are obtained from analysis of data from a broad range of processes. Precise knowledge of PDFs will be particularly important for analysis of data at the Large Hadron Collider (LHC) where new phenomena may be revealed via small deviations from Standard Model (SM) predictions. The Drell-Yan process [1], in which quark-antiquark annihilations form intermediate γ^* or Z (γ^*/Z) vector bosons decaying to lepton pairs, is particularly useful in providing information on PDFs at $Q^2 = M_{\ell\ell}^2$, where $M_{\ell\ell}$ is the invariant mass of the dilepton pair. In the leading order (LO) approximation, the momentum fractions x_1, x_2 carried by the initial state quarks in the proton and antiproton, respectively, are related to the rapidity y [2] of the γ^*/Z boson via the equation $x_{1,2} = (M_{\ell\ell}/\sqrt{s})e^{\pm y}$, where \sqrt{s} is the center of mass energy. Dilepton pairs produced at large y originate from collisions in which one parton carries a large and the other a small momentum fraction x . A measurement of $d\sigma/dy$ at large y tests PDFs at high x , a region not well constrained by current results. Therefore, precise measurements of W and Z boson rapidity distributions at the Tevatron determine the size of higher order QCD terms and can be used to further refine current PDF models. Furthermore since the Z production cross section is predicted with an accuracy of $\approx 2\%$ [3], precise measurements of the rate of Z production at the Tevatron and the LHC can be used to determine the integrated luminosity [4] more precisely than the traditional method of using the total inelastic cross section. This has particular applicability to sub-processes initiated by a quark and an anti-quark and can reduce the uncertainty in the determination of LHC and Tevatron cross sections.

The most recent Tevatron measurement of $d\sigma/dy$ for e^+e^- pairs in the Z boson mass region was performed

by the D0 [5] experiment, using a data-set corresponding to 0.4 fb^{-1} of integrated luminosity. Here, we report on a new measurement of $d\sigma/dy$ at the Tevatron with an integrated luminosity of 2.1 fb^{-1} . The measured rapidity range extends to $|y| \sim 2.9$, close to the kinematic limit of $|y| = 3.0$ for Z boson production at $\sqrt{s} = 1.96 \text{ TeV}$. The $d\sigma/dy$ distribution is compared to the predictions of perturbative QCD calculations in Next-to-Leading-Order (NLO) and Next-to-Next-to-Leading-Order (NNLO) with different PDF models.

II. EVENT SELECTION AND ANALYSIS METHOD

The data sample corresponds to an integrated luminosity of 2.1 fb^{-1} collected by the CDF II Detector at Fermilab [6] during 2004-2007. CDF II uses a 1.4 T solenoidal magnetic spectrometer surrounded by projective-tower-geometry calorimeters and outer muon detectors. Charged particle directions and momenta are measured by an open-cell drift chamber (COT), a silicon vertex detector (SVX), and an intermediate silicon layer (ISL). The coverage of COT tracking in pseudorapidity is $|\eta| < 1.2$ [2]. Reconstructed tracks are used to determine the $p\bar{p}$ collision point along the beam line (z_{vertex}), which is required to be within $z = \pm 60 \text{ cm}$ of the detector. The energies and directions [2] of electrons, photons, and jets are measured by two separate calorimeters: central ($|\eta| < 1.1$) and plug ($1.1 < |\eta| < 3.6$). Each calorimeter has an electromagnetic (EM) compartment with a shower maximum detector followed by a hadronic (HAD) compartment. Three topologies of e^+e^- pairs are considered: two central electrons (CC), one central and one plug electron (CP), and two plug electrons (PP). The inclusion of PP events allows the measurement of Z bosons in the forward rapidity region which corresponds to high and low parton momentum fractions.

Data are collected using a three-level trigger system [6] and trigger paths with either one central electron or two electrons (central or plug) with transverse energy $E_T > 18 \text{ GeV}$. Electron identification requirements [7] are imposed to select signal events and to suppress background. Both electron candidates are required to be isolated from any other calorimetric activity. The fraction of energy in the HAD calorimeter towers behind the EM shower is required to be small [7], as expected for an EM shower. Electron candidates with $E_T > 25 \text{ GeV}$ for CC and PP events, and $E_T > 20 \text{ GeV}$ for CP events, are selected in the central ($|\eta| < 1.1$), and plug ($1.2 < |\eta| < 2.8$) fiducial regions of the calorimeters. Central electron candidates must have a COT track that extrapolates to a shower cluster in the EM calorimeter and a track momentum consistent with the calorimeter measurement. Central and plug electron candidates are required to have EM-like transverse shower profiles using the shower maximum detectors. In order to reduce background we require that at least one of the plug elec-

Fukui Prefecture, Japan 910-0017, ^mKinki University, Higashi-Osaka City, Japan 577-8502, ⁿUniversidad Iberoamericana, Mexico D.F., Mexico, ^oUniversity of Iowa, Iowa City, IA 52242, ^pKansas State University, Manhattan, KS 66506, ^qQueen Mary, University of London, London, E1 4NS, England, ^rUniversity of Manchester, Manchester M13 9PL, England, ^sMuons, Inc., Batavia, IL 60510, ^tNagasaki Institute of Applied Science, Nagasaki, Japan, ^uUniversity of Notre Dame, Notre Dame, IN 46556, ^vObninsk State University, Obninsk, Russia, ^wUniversity de Oviedo, E-33007 Oviedo, Spain, ^xTexas Tech University, Lubbock, TX 79609, ^yIFIC(CSIC-Universitat de Valencia), 56071 Valencia, Spain, ^zUniversidad Tecnica Federico Santa Maria, 110v Valparaiso, Chile, ^{aa}University of Virginia, Charlottesville, VA 22906, ^{bb}Bergische Universität Wuppertal, 42097 Wuppertal, Germany, ^{cc}Yarmouk University, Irbid 211-63, Jordan, ^{kk}On leave from J. Stefan Institute, Ljubljana, Slovenia,

trons in PP events has a track reconstructed in the SVX that points to the EM cluster in the calorimeter. The efficiency of having at least one electron matched to an SVX track is about 85%. The selected number of CC, CP, and PP events with $66 < M_{ee} < 116 \text{ GeV}/c^2$ is 50752, 86203, and 31415, respectively.

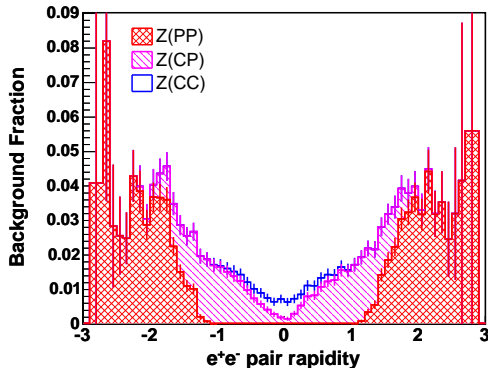


FIG. 1: The distribution of background events as a function of rapidity for CC, CP and PP e^+e^- candidates (shown as a fraction of all candidate events selected in this analysis). The error bars include the statistical and systematic uncertainty.

III. BACKGROUNDS

The main backgrounds are QCD dijet and photon plus jet events in the plug region (because of the limited tracking at large $|\eta|$). The jet background is measured separately in each e^+e^- pair topology by statistically separating electrons from jets on the basis of the transverse energy profile distributions in the calorimeter and the invariant mass distribution of e^+e^- pairs [7]. The distribution of background events as a function of rapidity for CC, CP and PP e^+e^- candidates (shown as a fraction of all candidate events selected in this analysis) is shown in Fig. 1. The fractional contribution of the total background to the number of selected events is $0.24 \pm 0.03\%$ (stat \oplus syst) for CC, $1.55 \pm 0.44\%$ for CP, and $3.40 \pm 0.75\%$ for PP events. The background from electroweak (WW , WZ , W +jets, and $Z \rightarrow \tau^+\tau^-$) and $t\bar{t}$ processes is estimated from simulation to be $0.41 \pm 0.02\%$.

IV. ACCEPTANCE AND EFFICIENCIES

The acceptance is defined as the ratio of the number of Monte Carlo (MC) simulation events that pass selection criteria in each y bin of the reconstructed final state e^+e^- pair (including resolution smearing) to the number of MC generated events in each true y bin of the generated γ^*/Z boson. The resolution in the measurement of the e^+e^- invariant mass is $2.2 \text{ GeV}/c^2$, and the resolution in the measurement of y is 0.015. The acceptance is modeled

using the PYTHIA [8] generator combined with a GEANT [11] simulation of the CDF detector.

The PYTHIA generator includes a LO QCD interaction ($q + \bar{q} \rightarrow \gamma^*/Z$), initial state QCD radiation, parton shower fragmentation, the $\gamma^*/Z \rightarrow e^+e^-$ decay, and photon radiation from the final state. The version of PYTHIA used at CDF has additional ad-hoc tuning [8] in order to accurately represent the Z boson transverse momentum distribution measured in data. To reconstruct the simulated events in the same way as data, the calorimetry energy scale, resolutions, and selection efficiencies used in the detector simulation are tuned using data.

Because the acceptance depends on modeling of the Z boson rapidity, transverse momentum and angular distributions of the electron pairs, it is important to correct for possible model dependences arising from the choice of the event generator or a particular PDF set. The uncorrected acceptance is calculated using the CTEQ5L [9] LO PDFs, and we compare relevant kinematic distributions in the MC simulation to those observed in the data to correct the acceptance for possible observed discrepancies.

While the generated rapidity spectrum is in good agreement with the data for $y < 2$, the data and simulation do not agree at larger values of y . To correct for this discrepancy, we modify the MC generated event spectrum (dN/dy) so that the final accepted MC spectrum matches the spectrum in data, as shown in Fig. 2. A comparison of the reconstructed transverse momentum spectra of the e^+e^- pairs in the data and the MC simulation reveals good agreement as shown in Fig. 3. Modifying the P_T spectrum in simulation to exactly follow the data leads to a negligible change in the calculated acceptance. A comparison of the average P_T of events in bins of y shows that the data is well modeled by the simulation. Similarly, a study of the angular distribution in θ (where θ is the polar angle of the final state electron in the Collins-Soper frame [10]) in data shows good agreement with the simulation as illustrated in Fig. 4.

The acceptance (A) and efficiencies (ϵ) are determined as a function of boson rapidity. The contributions of each topology to the product $A \times \epsilon$ are shown in Fig. 5.

V. DIFFERENTIAL AND TOTAL CROSS SECTIONS

The differential cross section is given by

$$\frac{d\sigma(\gamma^*/Z)}{dy}(y) = \frac{N_{sig}(y) - N_{bkg}(y)}{c(y)\Delta y \epsilon_{zvtx} \sum_i [(A_i \times \epsilon_i(y)) \epsilon_{trig}^i(y) \mathcal{L}_i]}$$

where $N_{sig}(y) - N_{bkg}(y)$ is the number of events after subtracting background, $c(y)$ is a correction factor used in order to yield $d\sigma/dy$ at the center of the bin, and Δy is the y bin size ($\Delta y = 0.1$ up to $y = 2.7$ and $\Delta y = 0.2$ for the last bin, $2.7 < y \leq 2.9$). The sum index i runs over the e^+e^- topologies (CC, CP, PP), $A_i \times \epsilon_i(y)$ is the combined acceptance and event selection efficiency,

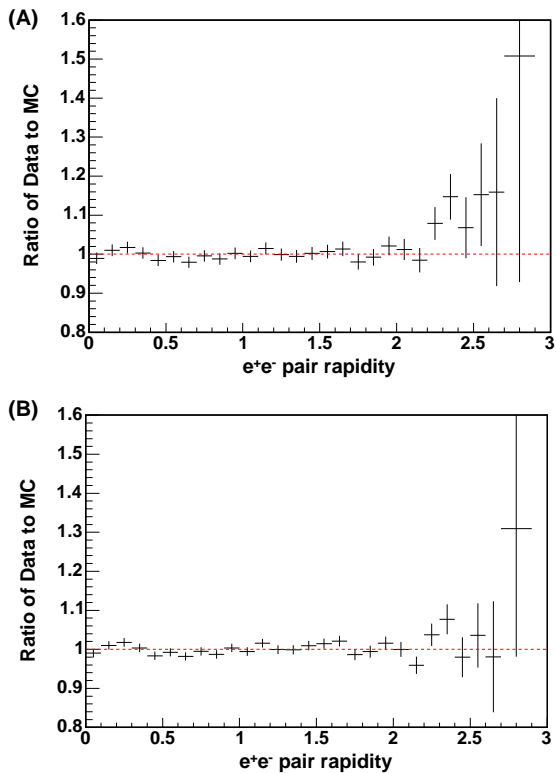


FIG. 2: The ratio of the rapidity distributions dN/dy of reconstructed e^+e^- pairs in data to the results from the simulation using PYTHIA, CTEQ5L LO PDFs and CDF W/Z tuning parameters [8]. (A) PYTHIA before modification of the rapidity distribution. (B) PYTHIA after modification of the rapidity distribution.

$\epsilon_{trig}^i(y)$ is the trigger efficiency, \mathcal{L}_i is the total integrated luminosity for each topology, and ϵ_{zvtx} is the acceptance for the $p\bar{p}$ collision vertex to occur within $z = \pm 60$ cm of the center of the detector. The ϵ_{zvtx} in the data taken before June 2006 is $95.8 \pm 0.2\%$ and after that is $96.8 \pm 0.2\%$.

Systematic uncertainties in $d\sigma/dy$ originate from uncertainties in the estimates of the acceptance, backgrounds, electron identification efficiency, SVX tracking efficiency, and modeling of material in the detector. Uncertainties associated with correcting the acceptance for differences between kinematic distributions in data and simulation are found to be negligible. The total systematic uncertainty is $\sim 1.0\%$ of $d\sigma/dy$ for $|y| < 2.5$, increasing to 10.0% at $|y| = 2.9$. The uncertainty on the integrated luminosity (lum.) is 6% .

VI. RESULTS

The measured $d\sigma/dy$ values, which are symmetric about $y = 0$, are shown versus $|y|$, with statistical and systematic uncertainties, in Fig. 6 and Table I. The

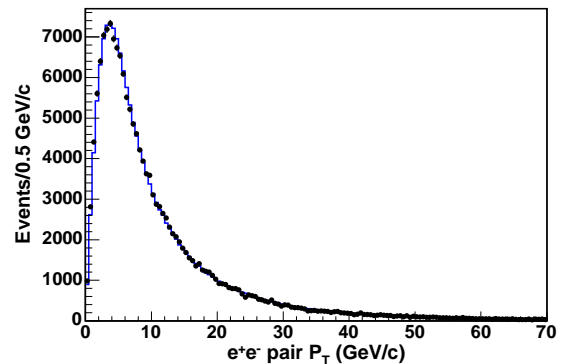


FIG. 3: The reconstructed transverse momentum distribution of e^+e^- pairs (after all event selection cuts) compared to the results from the simulation using PYTHIA, CTEQ5L LO PDFs and CDF W/Z tuning parameters [8]. The black points are data and the blue solid line is the PYTHIA MC prediction.

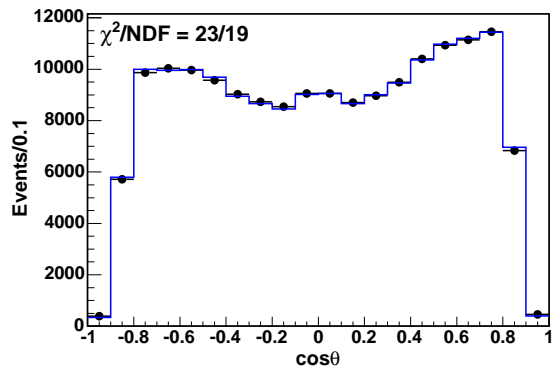


FIG. 4: The reconstructed polar angle distribution of e^+e^- pairs (after all event selection cuts) compared to the results from the simulation using PYTHIA, CTEQ5L LO PDFs and CDF W/Z tuning parameters [8]. The black points are data and the blue solid line is the PYTHIA MC prediction.

total cross section, derived from integrating $d\sigma/dy$ up to $|y| = 2.9$, is $\sigma = 256.6 \pm 0.7(\text{stat.}) \pm 2.0(\text{syst.}) \pm 15.4(\text{lum.})$ pb. These results are compared to QCD predictions at LO with CTEQ5L [9], at NLO [17] with MRST2001 (NLO) [14], MRST2004 (NLO) [15], CTEQ6.1M (NLO) [12], CTEQ6.6M (NLO) [13], and MSTW2008 (NLO) [3] PDFs, and at NNLO [18] with MRST2006E (NNLO) [16] and MSTW2008 (NNLO) [3] PDFs. The measured total cross section is consistent with both NLO and NNLO calculations as shown in Table II.

In comparing the shape of the measured $d\sigma/dy$ to theory, the latter distributions are normalized to the measured total cross section of 256.6 pb. The ratios of the measured $d\sigma/dy$ to the QCD calculations at LO, NLO and NNLO with the above mentioned PDFs are shown in Figures 7, 8, and 9. The yellow bands in the fig-

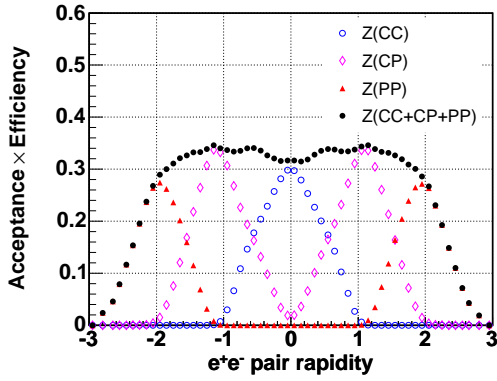


FIG. 5: The product of kinematic acceptance and event selection efficiency *vs.* the rapidity of the e^+e^- pair. The black points are the sum of all topologies.

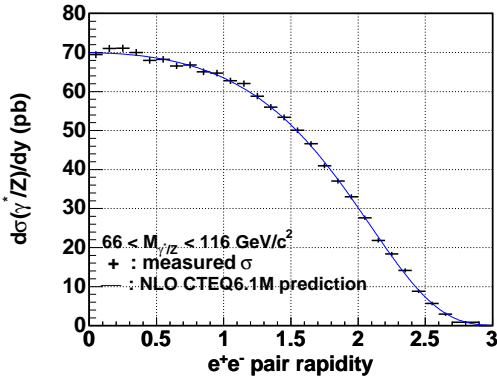


FIG. 6: The measured $d\sigma/dy$ for $p\bar{p} \rightarrow Z^0/\gamma^* \rightarrow e^+e^-$ over the entire rapidity range. The points are the measured cross section versus $|y|$ and the solid line is the theory prediction (scaled to the measured total cross section) for CTEQ6.1M(NLO) PDFs.

ures correspond to the uncertainties associated to the MSTW2008E (NLO and NNLO) PDFs, which are given with 68% C.L. errors and to the those associated to the other sets of PDFs, given with 90% C.L. errors. A χ^2 comparison (including statistical and systematic uncertainties) is shown in Table III. Better agreement is obtained for the MSTW (2008) PDF at NNLO compared to NLO. The NLO CTEQ6.1M, CTEQ6.6M, the NNLO MRST2006 and MSTW2008 PDFs all describe the data well. The older NLO MRST (2004) set provides a poorer description of the data and, as expected, so does the LO PDF, CTEQ5L. The MSTW(2008) PDF used a preliminary version of the data presented in this paper in their fit. The correlations [7, 19] between the uncertainties in different y bins are included in the χ^2 comparison.

In summary, high-statistics measurement of γ^*/Z production in the Z mass region and of its rapidity distribution are found to agree with theoretical calcula-

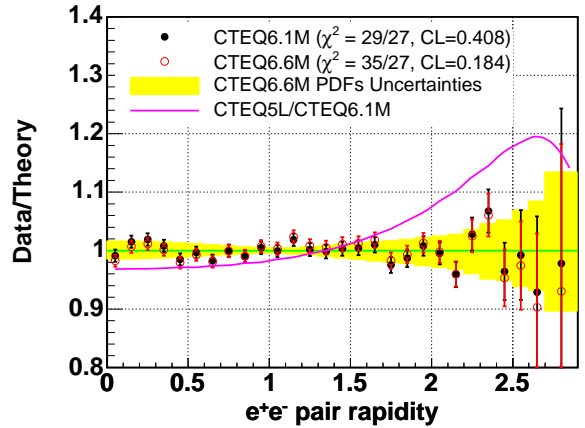


FIG. 7: The ratio of the experimental distribution of $d\sigma/dy$ (statistical and systematic uncertainties combined) to the theoretical predictions with CTEQ NLO PDFs (CTEQ6.1M and CTEQ6.6M). The yellow bands corresponds to the CTEQ6.6M PDFs 90% C.L. uncertainties. The χ^2 test includes the data statistical and systematic uncertainties.

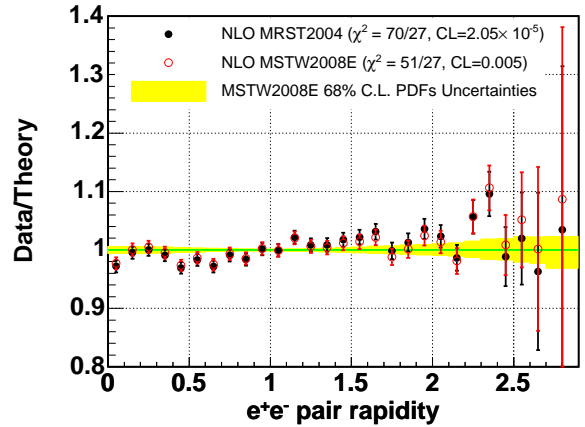


FIG. 8: The ratio of the experimental distribution of $d\sigma/dy$ (statistical and systematic uncertainties combined) to the theoretical predictions with MRST2004 and MSTW2008E NLO PDFs. The yellow bands corresponds to the MSTW2008E PDFs 68% C.L. uncertainties. The χ^2 test includes the data statistical and systematic uncertainties.

tions that use recent NLO and NNLO PDFs. (A preliminary version of these results has been used in the determination of the most recent PDFs). The precise measurement of the total production cross section, $\sigma = 256.6 \pm 0.7(\text{stat.}) \pm 2.0(\text{syst.}) \pm 15.4(\text{lum.})$ pb can be used to set the normalization of other processes at the Tevatron and the LHC.

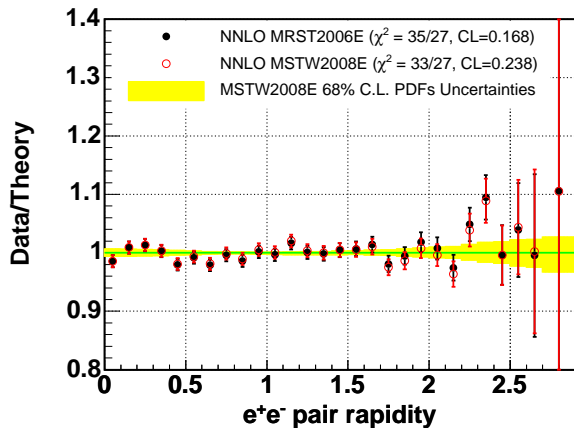


FIG. 9: The ratio of the experimental distribution of $d\sigma/dy$ (statistical and systematic uncertainties combined) to the theoretical predictions with MRST2006E and MSTW2008E NNLO PDFs. The yellow bands corresponds to the MSTW2008E PDFs 68% C.L. uncertainties. The χ^2 test includes the data statistical and systematical uncertainties.

TABLE I: Differential cross sections for production of e^+e^- pairs in the mass range $66 < M_{ee} < 116 \text{ GeV}/c^2$. The first and second uncertainties are statistical and systematical, respectively. The 6% luminosity uncertainty is not included. The quoted y values correspond to the center of the bin. The bin size is 0.1 up to $y = 2.7$ and 0.2 for the last bin.

y	$d\sigma/dy[\text{pb}]$	y	$d\sigma/dy[\text{pb}]$
0.05	$69.46 \pm 0.73 \pm 0.49$	1.55	$50.07 \pm 0.62 \pm 0.37$
0.15	$71.03 \pm 0.74 \pm 0.49$	1.65	$46.59 \pm 0.61 \pm 0.35$
0.25	$71.10 \pm 0.74 \pm 0.49$	1.75	$40.97 \pm 0.58 \pm 0.34$
0.35	$70.01 \pm 0.72 \pm 0.48$	1.85	$37.04 \pm 0.56 \pm 0.33$
0.45	$67.97 \pm 0.70 \pm 0.47$	1.95	$33.02 \pm 0.55 \pm 0.31$
0.55	$68.22 \pm 0.70 \pm 0.47$	2.05	$27.65 \pm 0.52 \pm 0.25$
0.65	$66.58 \pm 0.69 \pm 0.47$	2.15	$21.84 \pm 0.49 \pm 0.23$
0.75	$66.81 \pm 0.70 \pm 0.48$	2.25	$18.35 \pm 0.50 \pm 0.20$
0.85	$65.05 \pm 0.69 \pm 0.49$	2.35	$14.13 \pm 0.49 \pm 0.17$
0.95	$64.70 \pm 0.69 \pm 0.50$	2.45	$8.80 \pm 0.45 \pm 0.10$
1.05	$62.74 \pm 0.67 \pm 0.50$	2.55	$5.68 \pm 0.44 \pm 0.09$
1.15	$62.02 \pm 0.66 \pm 0.49$	2.65	$2.93 \pm 0.41 \pm 0.15$
1.25	$58.80 \pm 0.65 \pm 0.48$	2.80	$0.87 \pm 0.22 \pm 0.11$
1.35	$56.02 \pm 0.65 \pm 0.43$	2.95	—
1.45	$53.37 \pm 0.63 \pm 0.40$		

Acknowledgments

We thank the Fermilab staff and the technical staffs of the participating institutions for their vital contribu-

tions. This work was supported by the U.S. Department of Energy and National Science Foundation; the Italian Istituto Nazionale di Fisica Nucleare; the Ministry of Education, Culture, Sports, Science and Technology of Japan; the Natural Sciences and Engineering Research Council of Canada; the National Science Council of the

TABLE II: A comparison of the measured total cross section for the production of e^+e^- pairs in the mass range $66 < M_{ee} < 116 \text{ GeV}/c^2$ to theory calculations.

<i>Model</i>	<i>Total cross section</i>
CTEQ5L(LO)	183.3
MRST2001E(NLO)	$241.0^{+2.8}_{-3.4}$
MRST2004(NLO)	241.2
MSTW2008E(NLO)	$242.6^{+4.6}_{-5.5}$
CTEQ6.1M(NLO)	$236.1^{+9.3}_{-9.2}$
CTEQ6.6M(NLO)	$238.7^{+7.1}_{-7.0}$
MRST2006E(NNLO)	$251.6^{+2.8}_{-3.1}$
MSTW2008E(NNLO)	$248.7^{+5.1}_{-4.0}$
Data	$256.6 \pm 0.7 \pm 2.0 \pm 15.4$

TABLE III: A comparison of the shape of the measured $d\sigma/dy$ distribution to theoretical predictions with several choices of PDFs. The theoretical distributions are normalized to the measured total cross section of 256.6 pb. The χ^2 for 27 degrees of freedom includes statistical and systematic uncertainties.

<i>Model</i>	χ^2/DOF	<i>CL</i>
CTEQ5L(LO)	242/27	—
MRST2001E(NLO)	76/27	2.908×10^{-6}
MRST2004(NLO)	70/27	2.049×10^{-5}
MSTW2008E(NLO)	51/27	0.005
CTEQ6.1M(NLO)	29/27	0.408
CTEQ6.6M(NLO)	35/27	0.184
MRST2006E(NNLO)	35/27	0.168
MSTW2008E(NNLO)	33/27	0.238

Republic of China; the Swiss National Science Foundation; the A.P. Sloan Foundation; the Bundesministerium für Bildung und Forschung, Germany; the World Class University Program, the National Research Foundation of Korea; the Science and Technology Facilities Council and the Royal Society, UK; the Institut National de Physique Nucleaire et Physique des Particules/CNRS; the Russian Foundation for Basic Research; the Ministerio de Ciencia e Innovación, and Programa Consolider-Ingenio 2010, Spain; the Slovak R&D Agency; and the Academy of Finland. We also thank Robert Thorne for valuable discussions.

- [1] S.D. Drell and T.-M. Yan, Phys. Rev. Lett. **25**, 316 (1970).
[2] CDF coordinates are (θ, ϕ, z) , where θ is the polar an-

gle relative to the proton beam (the $+z$ axis), and ϕ the azimuth. The pseudorapidity is $\eta = -\ln \tan(\theta/2)$. For an $e^+ + e^-$ pair $P_T = P \sin \theta$, $E_T = E \sin \theta$, and

- $y = \frac{1}{2} \ln \frac{E+P_z}{E-P_z}$, where P and P_z are the magnitude and z component of the momentum, and E is the energy of the $e^+ + e^-$ pair.
- [3] A.D. Martin, W.J. Stirling, R.S. Thorne, G. Watt, *Eur. Phys. J.* **C63**, 189 (2009).
- [4] M. Dittmar, F. Pauss and D. Zurcher, *Phys. Rev.* **D56**, 7284 (1997). V.A. Khoze, A.D. Martin, R. Orava and M.G. Ryskin. *Eur. Phys. J.* **C19**, 313 (2001).
- [5] V.M. Abazov *et al.*, (*D0* collaboration), *Phys. Rev.* **D76**, 012003 (2007).
- [6] The CDF II Detector Technical Design Report, Fermilab-Pub-96/390-E; D. Amidei *et al.*, *Nucl. Instrum. Methods Phys. Res.* **A350**, 73 (1994); F. Abe *et al.*, *Phys. Rev.* **D52**, 4784 (1995); P. Azzi *et al.*, *Nucl. Instrum. Methods Phys. Res.* **A360**, 137 (1995); D. Acosta *et al.* (*CDF* Collaboration), *Phys. Rev.* **D71**, 032001 (2005).
- [7] Jiyeon Han, PhD Thesis, University of Rochester, FERMILAB-THESIS-2008-65.
- [8] T. Sjöstrand *et al.*, *JHEP05(2006)026*. We use the default (MSEL=11) LO matrix element ($Z + 0$ jet) with CTEQ5L PDFs and electroweak coupling $\sin^2 \theta_W = 0.232$. The parton showering produces the boson P_T . The CDF EWK/TOP standard W/Z P_T tuning parameters are: MSTP(91)=1, PARP(91)=2.10, PARP(93)=15 for the low P_T Gaussian smearing, with PART(62)=1.25 and PARP(62)=0.2 for the P_T evolution in 7-25 *GeV* region. The underlying event is included as Tune A.
- [9] H. L. Lai *et al.*, *Eur. Phys. J.* **C12**, 375 (2000).
- [10] J. C. Collins and D. E. Soper, *Phys. Rev.* **D16**, 2219 (1977).
- [11] GEANT: CERN Program Library Long Writeup W5013 (1993).
- [12] J. Pumplin, D.R. Stump, J. Huston, H.L. Lai, P.Nadolsky, W.K. Tung, *JHEP* 0207 (2002) 012; J. Pumplin, D.R. Stump, J. Huston, H.L. Lai, W.K. Tung, S. Kuhlmann, J.F. Owens, *JHEP* 0310:046 (2003).
- [13] P.Nadolsky, H.L. Lai, Q.H. Cao, J. Huston, J. Pumplin, D. Stump, W.K. Tung, and C.P. Yuan, *Phys. Rev.* **D78**, 013004 (2008).
- [14] A.D. Martin, R.G. Roberts, W.J. Stirling, and R.S. Thorne, *Eur. Phys. J.* **C28**, 455 (2003).
- [15] A.D. Martin, R.G. Roberts, W.J. Stirling, and R.S. Thorne, *Phys. Lett.* **B604**: 61-68 (2004).
- [16] A.D. Martin, W.J. Stirling, R.S. Thorne, and G. Watt, *Phys. Lett.* **B652**, 292 (2007).
- [17] P.J. Sutton, A.D. Martin, R.G. Roberts, and W.J. Stirling, *Phys. Rev.* **D45**, 2349 (1992).
- [18] P.J. Rijken, W.L. van Neerven, *Phys. Rev.* **D51**, 44 (1995); \overline{MS} NNLO for $d^2\sigma/dy dM$: C. Anastasiou, L. Dixon, K. Melnikov, and F. Petriello, *Phys. Rev.* **D69**, 094008 (2004).
- [19] CERN ROOT and C++ code for $d\sigma/dy$ and statistical and systematic uncertainty contributions from each source including correlations is available at http://www-cdf.fnal.gov/physics/ewk/2009/dszdy/dszdy_sys.htm